



6-2-14

## BEHAVIOR OF TUBULAR COLUMN TO H-BEAM CONNECTIONS UNDER SEISMIC LOADING

Mototsugu TABUCHI, Hiroshi KANATANI and Teruyasu KAMBA

Department of Architecture, Faculty of Engineering, Kobe University,  
Nada-ku, Kobe, Japan

### SUMMARY

This paper describes the behavior of joint panels of hollow-section column to H-beam connections in moment-resisting steel frames under lateral force. From the tests on many connection assemblages with various diameter-to-thickness ratios ( $D/T$ ) and axial load ratios ( $N/N_y$ ) of columns, the following are shown: (1) To insure the sufficient strength and deformation capacity of the joint panels, the connections should be stiffened adequately for the local failure. (2) In the connections with  $D/T < 30$ , the hysteresis loops are stable and large plastic deformation can be expected. In the connections with  $D/T > 40$ , the deformation capacity is poor due to premature shear buckling of the joint panels. (3) In the connections with  $N/N_y > 0.3$ , large plastic deformations cannot be expected even in the case of  $D/T \approx 30$ .

### INTRODUCTION

In moment-resisting steel frames under lateral force, joint panels of column to beam connections are deformed by high shear stress. Therefore, it is very important problem for aseismic design of the frames to study the strength and plastic deformation capacity of the joint panels. Extensive studies (Refs.1,2,3 etc.) have been carried out on the behaviors of H-column to H-beam connections, but the studies on hollow-section column to H-beam connections are limited (Refs.4,5 etc.).

In hollow-section column connections stiffened by exterior diaphragms, the local failure of connections must be taken into account as well as the shear failure of joint panels. Here, the local failure means the failure mode of connections caused by the deformation of column walls under normal forces from beam flanges.

This paper presents the behaviors of rectangular and circular hollow-section (RHS and CHS) column to H-beam connections with various diameter-to-thickness ratios ( $D/T$ ) and axial load ratios ( $N/N_y$ ) of the columns.

### TESTS

Specimens Thirty nine connection assemblages were tested. The columns are cold-rolled tubes except two RHS column specimens built-up by four steel plates (\* in Table 1). The connections are stiffened by exterior diaphragms at the beam flange

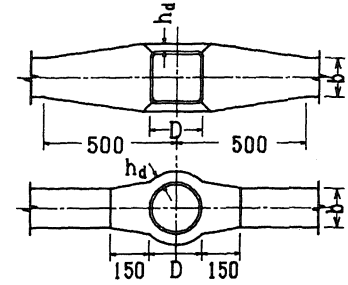
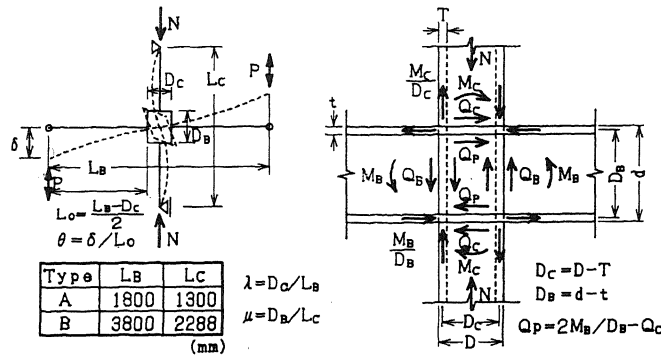


Fig.1 Schematic Diagram of Test Set-up and Nomenclature

Fig.2 Details of Diaphragms

Table 1 Details of Test Specimens

| Specimen | Column<br>DxDxT, DxT | Beam<br>d x b x tw x t | Diaphragm     |    | D/T | Axial<br>force<br>N/Ny | Column     |            | Diaphragm  |            | Specimen<br>type |   |
|----------|----------------------|------------------------|---------------|----|-----|------------------------|------------|------------|------------|------------|------------------|---|
|          |                      |                        | td            | hd |     |                        | $\sigma_y$ | $\sigma_u$ | $\sigma_y$ | $\sigma_u$ |                  |   |
| RHS      | BX17-0.2             | 200x200x12             | 300x150x9 x12 | 12 | 40  | 17                     | 0.20       | 3.81       | 4.42       | 3.15       | 4.73             | A |
|          | BX22-0               | 200x200x 9             | 300x150x9 x12 | 12 | 40  | 22                     | 0          | 4.20       | 5.14       | 2.78       | 4.45             | A |
|          | BX22-0.2             | 200x200x 9             | 300x150x9 x12 | 12 | 40  | 22                     | 0.20       | 4.20       | 5.14       | 2.99       | 4.75             | A |
|          | BX22B-0.2            | 200x200x 9*            | 300x150x9 x12 | 12 | 40  | 22                     | 0.20       | 3.16       | 4.76       | 2.78       | 4.45             | A |
|          | BX22B-0.4            | 200x200x 9*            | 300x150x9 x12 | 12 | 40  | 22                     | 0.40       | 3.16       | 4.76       | 2.99       | 4.75             | A |
|          | BX33-0.2             | 200x200x 6             | 300x150x6.5x9 | 9  | 40  | 33                     | 0.18       | 3.43       | 4.37       | 3.20       | 4.66             | A |
|          | BX33-0.4             | 200x200x 6             | 300x150x6 x 9 | 9  | 40  | 33                     | 0.40       | 3.90       | 4.70       | 2.88       | 4.41             | A |
|          | BX42-0               | 250x250x 6             | 350x175x7 x11 | 12 | 60  | 42                     | 0          | 3.33       | 4.62       | 2.99       | 4.75             | B |
| BX44-0.2 | 200x200x4.5          | 300x150x6.5x9          | 9             | 40 | 44  | 0.18                   | 3.29       | 4.23       | 3.20       | 4.66       | A                |   |
| CHS      | CL27-0               | 216.3φx 8              | 300x150x6.5x9 | 12 | 45  | 27                     | 0          | 4.44       | 4.87       | 2.97       | 4.42             | B |
|          | CL27-0.3†            | 216.3φx 8              | 300x150x6.5x9 | 12 | 45  | 27                     | 0.33       | 4.44       | 4.87       | 2.97       | 4.42             | B |
|          | CL36-0               | 216.3φx 6              | 300x150x6.5x9 | 12 | 45  | 36                     | 0          | 3.32       | 3.98       | 3.15       | 4.73             | B |
|          | CL45-0               | 318.5φx 7              | 400x200x8 x13 | 16 | 70  | 45                     | 0          | 5.20       | 5.63       | 2.85       | 4.54             | B |
|          | CL48-0               | 216.3φx4.5             | 300x150x6.5x9 | 9  | 45  | 48                     | 0          | 3.96       | 4.70       | 2.88       | 4.41             | B |
|          | CL48-0.3†            | 216.3φx4.5             | 300x150x6.5x9 | 9  | 45  | 48                     | 0.33       | 3.96       | 4.70       | 2.88       | 4.41             | B |

\*:RHS built up by four plates †: Monotonous loads applied

Table 2 Summary of Test Results

| Specimen | Experiment     |                  |                |                  |                  | Calculation     |                 |                 |                 | M <sub>ly</sub> | M <sub>y</sub> | Failure<br>mode *) |   |
|----------|----------------|------------------|----------------|------------------|------------------|-----------------|-----------------|-----------------|-----------------|-----------------|----------------|--------------------|---|
|          | M <sub>y</sub> | M <sub>max</sub> | θ <sub>y</sub> | θ <sub>max</sub> | Y <sub>max</sub> | M <sub>py</sub> | M <sub>ly</sub> | M <sub>by</sub> | M <sub>cy</sub> |                 |                |                    |   |
| RHS      | BX17-0.2       | 15.3             | 20.8           | 1.10             | 11.2             | 10.6            | 16.6            | 18.2            | 19.0            | 21.9            | 1.10           | 0.92               | P |
|          | BX22-0         | 13.4             | 18.6           | 1.24             | >10.0            | > 9.1           | 14.2            | 13.9            | 16.8            | 19.4            | 0.98           | 0.94               | P |
|          | BX22-0.2       | 12.8             | 18.6           | 1.06             | >11.1            | >10.9           | 13.9            | 14.8            | 18.0            | 19.4            | 1.06           | 0.92               | P |
|          | BX22B-0.2      | 9.7              | 19.6           | 0.68             | >13.1            | >14.8           | 10.5            | 14.8            | 16.8            | 18.0            | 1.41           | 0.92               | P |
|          | BX22B-0.4      | 9.4              | 18.0           | 0.75             | >12.8            | >13.8           | 9.8             | 14.8            | 18.0            | 18.0            | 1.51           | 0.96               | C |
|          | BX33-0.2       | 8.2              | 11.6           | 1.01             | 6.1              | 5.1             | 7.8             | 9.1             | 16.5            | 11.2            | 1.16           | 1.05               | P |
|          | BX33-0.4       | 7.0              | 8.1            | 0.83             | 2.1              | 1.2             | 8.3             | 8.6             | 15.4            | 12.8            | 1.03           | 0.84               | P |
|          | BX42-0         | 10.6             | 12.5           | 1.08             | 3.0              | 1.9             | 10.1            | 15.8            | 23.2            | 16.7            | 1.56           | 1.05               | P |
| BX44-0.2 | 5.4            | 6.8              | 1.02           | 5.4              | -                | 5.7             | 7.4             | 15.4            | 8.5             | 1.31            | 0.96           | P                  |   |
| CHS      | CL27-0         | 12.2             | 14.9           | 1.91             | 13.8             | 8.8             | 11.3            | 15.9            | 18.3            | 16.7            | 1.41           | 1.08               | P |
|          | CL27-0.3       | 10.8             | 12.9           | 1.67             | 6.1              | 3.2             | 10.6            | 15.9            | 18.3            | 13.9            | 1.50           | 1.01               | C |
|          | CL36-0         | 6.2              | 8.1            | 1.34             | 9.1              | 7.5             | 6.4             | 9.0             | 18.4            | 9.5             | 1.41           | 0.97               | P |
|          | CL45-0         | 21.7             | 25.9           | 1.37             | 3.4              | 1.8             | 24.4            | 33.9            | 43.7            | 22.4            | 1.39           | 0.89               | P |
|          | CL48-0         | 5.1              | 6.1            | 1.18             | 4.1              | 4.1             | 5.8             | 7.2             | 18.4            | 8.7             | 1.24           | 0.88               | P |
|          | CL48-0.3       | 4.3              | 5.4            | 1.17             | 3.9              | 2.2             | 5.4             | 7.2             | 18.4            | 7.2             | 1.33           | 0.79               | C |

\*) P: Panel shear failure C: Column failure  
M<sub>y</sub>: Yield strength M<sub>max</sub>: Maximum strength M<sub>py</sub>: Panel yield strength  
M<sub>ly</sub>: Local yield strength M<sub>by</sub>: Beam yield strength M<sub>cy</sub>: Column yield strength  
θ<sub>y</sub>: Deformation at M<sub>y</sub> θ<sub>max</sub>: Deformation at M<sub>max</sub>  
Y<sub>max</sub>: Shear deformation of panel at M<sub>max</sub>

levels as shown in Fig.2. Each beam is proportioned to avoid the beam failure.

Table 1 shows the characteristics of fifteen specimens of which behaviors of the joint panels will be discussed in later. The other specimens, which were prepared for examining the effect of the local failure on the strength of connection assemblages, were omitted from Table 1 because of space limitations. The characteristics of the omitted specimens similar to those in Table 1 except that the diaphragm dimensions are smaller.

A schematic diagram of the test set-up is shown in Fig.1. A few cyclic loads (P) were statically applied in a testing frame except two CHS specimens applied monotonous loads († in Table 1).

**Test Results** Three failure modes were observed.

(a) Panel failure: At a joint panel, excessive shear deformation continued until the deformation was limited by the maximum jack stroke (the measured maximum load was regarded as the maximum strength (Mmax)), or the shear buckling occurred and the assemblages reached the maximum strength.

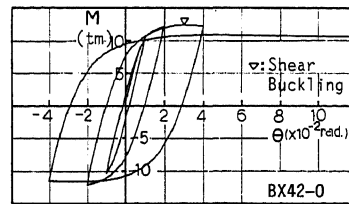
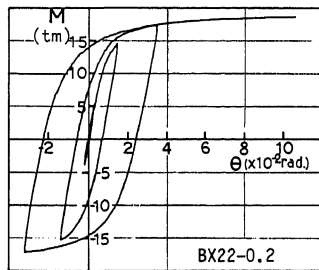
(b) Column failure: A column buckled locally due to a high axial load ratio (N/Ny).

(c) Local failure of connection: Excessive deformation of column walls occurred due to a lack of the stiffness of exterior diaphragms.

A summary of test results of the specimens listed in Table 1 is shown in Table 2, where calculated strengths are also indicated. For those specimens, the panel failure or the column failure was observed. The shear buckling was observed in the RHS column connections with  $D/T \geq 33$  and every CHS column connection.

The specimens omitted from Table 1 failed mainly according to the local failure.

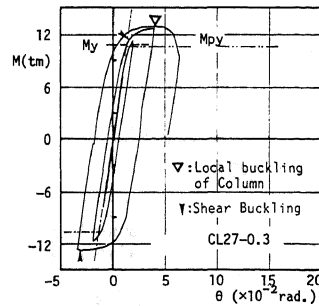
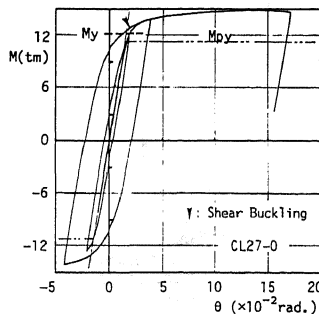
Typical load-deflection curves are shown in Figs.3 and 4, where the load (M) is represented in a bending moment corresponding with  $M_B$  in Fig.1, and  $\theta (= \delta/L_0)$



(a)

(b)

Fig.3 Load-Deflection Curves of RHS-Column Connections



(a)

(b)

Fig.4 Load-Deflection Curves of CHS-Column Connections

is equivalent to the story drift if  $L_c$  in Fig.1 is a story height. The experimental yield load ( $M_y$ ) is a general yield load obtained from the  $M-\theta$  curve. For the RHS column connections:

The hysteresis loops of the column with  $D/T=22$  were stable. On the other hand, in the column with  $D/T=42$ , the load could not exceed the maximum load attained in the previous loading cycles after the panel shear buckling had taken place (Fig.3)

For the CHS column connections:

The deformation capacity of the column with  $N/N_y=0.3$  was less than that without the axial load because of the column local buckling (Fig.4).

#### EFFECT OF LOCAL FAILURE ON SHEAR STRENGTH OF JOINT PANELS

Shear Yield Strength of Joint Panels The shear yield strength of joint panels can be predicted by a simplified stress analysis, assuming the equilibrium shown in Fig.1 and the von Mises's yield condition. In hollow-section columns, that is expressed in Eq.(1), where the shear strength ( $M_{py}$ ) is represented in a bending moment corresponding to  $M_B$  in Fig.1.

$$M_{py} = \frac{\sigma_{yc}}{\sqrt{3}} V_p \sqrt{1 - \left(\frac{N}{N_y}\right)^2 \frac{(1-\lambda)}{(1-\lambda-\mu)}} \quad (1)$$

where,  $\sigma_{yc}$ =yield stress of column

$$V_p = \frac{8}{9} D_B D_c T \quad \text{for RHS column}$$

$$V_p = \frac{\pi}{4} D_B D_c T \quad \text{for CHS column}$$

Local Yield Strength of Connection In hollow-section column connections stiffened by exterior diaphragms (Fig.2), the local failure may occur before the panel failure if the dimensions of exterior diaphragms are inadequate.

The authors proposed the empirical formulae for predicting the local strengths of RHS and CHS column connections in Refs.6 and 7. The local yield strengths of the connections from the proposal formulae can be expressed in Eqs.(2) and (3) with the same representation as Eq.(1).

$$\text{For RHS; } M_{LY} = 2.23 \sigma_{ud} \left(\frac{T}{D}\right)^{2/3} \left(\frac{td}{hd+T}\right)^{2/3} \left(\frac{hd+T}{D}\right)^2 D_B^2 \quad (2)$$

$$\text{For CHS; } M_{LY} = 0.65 \sigma_{yc} \left(\frac{5.13b+2.15}{D}\right) \left(\frac{T}{R}\right)^{0.863} \left(\frac{td}{R}\right)^{0.579} \left(\frac{hd+T}{R}\right)^{0.416} R^2 D_B \quad (3)$$

where,  $\sigma_{ud}$ =tensile strength of diaphragm  
 $R = (D-T)/2$

Discussion Figure 5 shows the effect of the local yield strength ( $M_{LY}$ ) on the yield strength ( $M_y$ ). It can be seen that  $M_{LY}$  is useful for predicting whether a connection assemblage will fail before the panel failure or not. Namely, the connection details must satisfy the condition of  $M_{LY}/M_{py} > 1.0$  to prevent premature local failure.

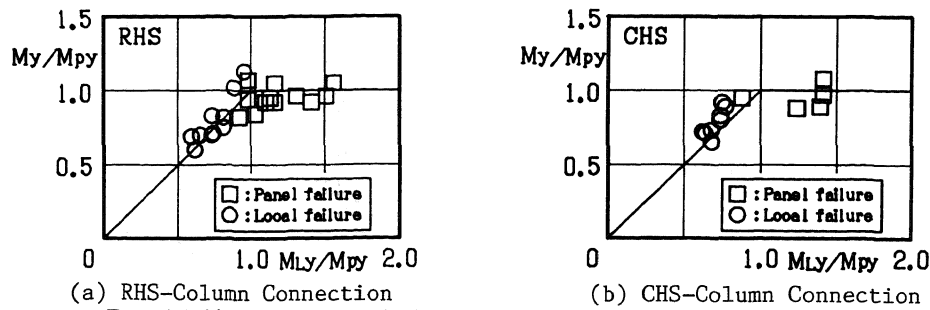


Fig.5 Effects of Local Yield on Yield Strength of Connections

## BEHAVIOR OF JOINT PANEL

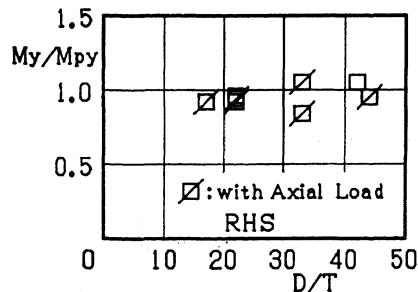
The behaviors of fifteen specimens with  $M_Ly/M_{py} > 1.0$ , shown in Tables 1 and 2, will be discussed.

**Yield Strength** Figure 6 shows the relationships between the  $M_y/M_{py}$  ratio and the  $D/T$  ratio. It is shown that the yield strength of joint panels can be predicted by Eq.(1). The mean value ( $m$ ) and the coefficient of variation ( $V$ ) are: for the RHS columns  $m=0.97$ ,  $V=0.07$ , and for the CHS columns  $m=0.94$ ,  $V=0.11$ . In the CHS columns, the  $M_y/M_{py}$  ratio decreases as the  $D/T$  ratio increases. On the other hand, the correlation between the  $M_y/M_{py}$  ratio and the  $D/T$  ratio cannot be seen in the RHS columns.

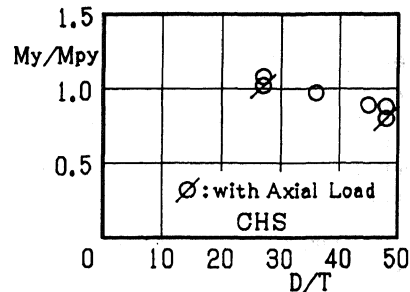
**Inelastic Behavior** Figure 7 shows the monotonic curves of the shear stress ( $\tau$ ) versus the shear strain ( $\gamma$ ) relationships in the joint panels. The ordinate and abscissa of the figure are indicated by the non-dimensional quantity  $\tau/\tau_y$  and  $\gamma/\gamma_y$  respectively, where  $\tau=2Q_p/A_p$  ( $A_p$ =cross-sectional area of column),  $\tau_y=\sigma_{yc}/\sqrt{3}$  and  $\gamma_y=\tau_y/G$ . The maximum shear stress of each specimen is indicated by a white circle in Fig.7.

The  $\tau_{max}/\tau_y$  ratios of the cold-rolled columns are from 1.0 to 1.3. The ratios of the built-up RHS columns are 1.5 and 1.6. These values are less than  $\tau_{max}/\tau_y$  ratios of H-columns (1.7 ~ 2.5) reported in Ref.3. The reasons of this phenomenon can be explained as follows:

- (a) Cold-rolled tubes have higher yield stress and yield ratio due to work-hardening through manufacturing process (Ref.8).
- (b) In hollow-section columns, the rigidity of the column flanges as a framing of the joint panels to restrict the plastic shear deformation is less than that of H-column flanges.

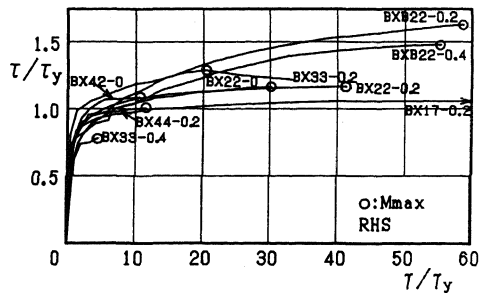


(a) RHS-Column Connection

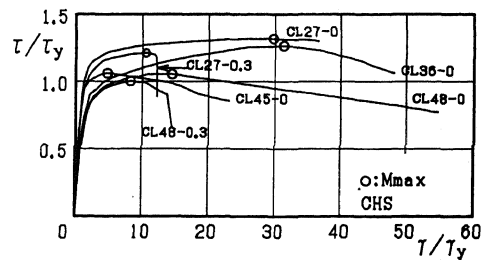


(b) CHS-Column Connection

Fig.6 Comparison between Observed and Calculated Yield Strength



(a) RHS-Column Connections



(b) CHS-Column Connections

Fig.7 Shear Stress versus Shear Strain Relationships

Deformation Capacity The relationship between the deformation capacity ( $\theta_{max}/\theta_y$ ) and the D/T ratio is shown in Fig.8. The  $\theta_{max}/\theta_y$  ratio decreases as the D/T ratio increases. For both of the RHS and CHS columns with D/T > 40, the  $\theta_{max}/\theta_y$  ratios are less than five. If the N/N<sub>y</sub> ratio is larger than one third, the  $\theta_{max}/\theta_y$  ratios are less than four even in the case of D/T=30.

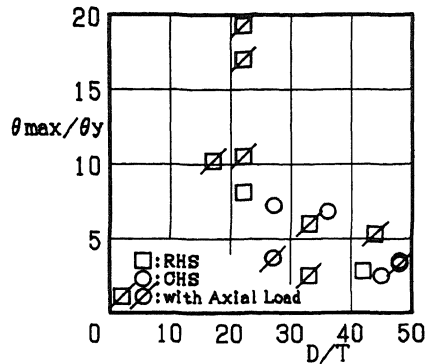


Fig.8 Relationship between  $\theta_{max}/\theta_y$  and D/T Ratio

#### REFERENCES

1. Fielding, D. J., and Huang, J. S., "Shear in Beam-to-Column Connections," The Welding Journal, Vol.50, (1971)
2. Bertero, V. V., Popov, E. P., and Krawinkler, H., "Beam-to-Column Subassemblages under Repeated Loading," Proceedings, ASCE, Vol.98 ST5, (1972)
3. Kato, B., "Beam-to-Column Connection Research in Japan," Proceedings, ASCE, Vol.108 ST2, (1982)
4. Tanaka, H., et al., "Limit analysis of Beam-Column Connections," Transaction of AIJ, No.163, 165, 166, 170, 174, (1969, 1970)
5. Kato, B., Maeda, Y., and Sakae, K., "Behavior of Rigid Frame Sub-Assemblages Subjected to Horizontal Force," Proceedings of International Conference held in Teesside Polytechnic, Joints in Structural Steelwork, (1980)
6. Tabuchi, M., Kanatani, H., Fujiwara, K., and Kamba, T., "On the Local Failure of Welded RHS-Column to H-Beam Connections," Proceedings of IIW International Conference held in Boston, Welding of Tubular Structures, (1984)
7. Kamba, T., Kanatani, H., Fujiwara, K., and Tabuchi, M., "On the Local Failure of Tubular Column to H-Beam Connections in Steel Structures," Proceedings of International Conference held in Teesside Polytechnic, Joints in Structural Steelwork, (1980)
8. Kato, B., Aoki, H., and Narihara, H., "Residual Stresses in Square Steel Tubes Introduced by Cold Forming and the Influence on Mechanical Properties," Proceedings of IIW International Meeting held in Tokyo, Safety Criteria in Design of Tubular Structures, (1986)